AJNR

Incorporating Functional MR Imaging into Diffusion Tensor Tractography in the Preoperative Assessment of the Corticospinal Tract in Patients with Brain Tumors

M. Smits, M.W. Vernooij, P.A. Wielopolski, A.J.P.E. Vincent, G.C. Houston and A. van der Lugt

AJNR Am J Neuroradiol 2007, 28 (7) 1354-1361
doi: https://doi.org/10.3174/ajnr.A0538
http://www.ajnr.org/content/28/7/1354

ORIGINAL RESEARCH

Incorporating Functional MR Imaging into Diffusion Tensor Tractography in the Preoperative Assessment of the Corticospinal Tract in Patients with Brain Tumors

M. Smits
M.W. Vernooij
P.A. Wielopolski
A.J.P.E. Vincent
G.C. Houston
A. van der Lugt

BACKGROUND AND PURPOSE: Our goal was to improve the preoperative assessment of the corticospinal tract (CST) in patients with brain tumors. We investigated whether the integration of functional MR imaging (fMRI) data and diffusion tensor (DT) tractography can be used to evaluate the spatial relationship between the hand and foot fibers of the CST and tumor borders.

MATERIALS AND METHODS: We imaged 10 subjects: 1 healthy volunteer and 9 patients. Imaging consisted of a 3D T1-weighted sequence, a gradient-echo echo-planar imaging (EPI) sequence for fMRI, and a diffusion-weighted EPI sequence for DT tractography. DT tractography was initiated from a seed region of interest in the white matter area subjacent to the maximal fMRI activity in the precentral cortex. The target region of interest was placed in the cerebral peduncle.

RESULTS: In the healthy volunteer, we successfully tracked hand, foot, and lip fibers bilaterally by using fMRI-based DT tractography. In all patients, we could track the hand fibers of the CST bilaterally. In 4 patients who also performed foot tapping, we could clearly distinguish hand and foot fibers. We were able to depict the displacement of hand and foot fibers by tumor and the course of fibers through areas of altered signal intensity.

CONCLUSION: Incorporating fMRI into DT tractography in the preoperative assessment of patients with brain tumors may provide additional information on the course of important white matter tracts and their relationship to the tumor. Only this approach allows a distinction between the CST components, while visualization of the CST is improved when fiber tracking is hampered by tumor (infiltration) or perifocal edema.

Blood oxygen-level dependent (BOLD) functional MR imaging (fMRI) is the most widely used noninvasive technique to identify the location of the cortical primary motor areas (PMA) preoperatively.[1-3] The site of activation on BOLD-fMRI has been proved to correlate well with the site at which intraoperative cortical stimulation identifies the PMA.[3-5] Therefore, fMRI information is used increasingly by neurosurgeons to plan their surgical procedures to maximize resection of tumor tissue while preserving eloquent brain areas.[6,7] However, neither fMRI nor anatomic MR images provide information on the (invisible) course of the important subcortical and deep white matter tracts, such as the corticospinal tract (CST). Inadvertent transection of CST fibers may have devastating results for the patient.[8] Therefore, visualization of the different components of the CST would provide important additional information for the preoperative assessment.

Diffusion tensor imaging (DTI) is a relatively new MR imaging technique that provides information on the microstructural organization of white matter in vivo and is a promising tool for the reliable preoperative assessment of the major white matter tracts in patients with brain tumors.[9-13] With DTI, the preferential diffusion of water molecules in the direction parallel to the orientation of white matter fibers makes it possible to visualize fiber tracts in 3D, by choosing seed and target regions of interest on the path of the fibers.[14,15] Until now, these regions of interest have almost exclusively been chosen on the basis of anatomic landmarks by using a DTI-based white matter atlas.[16-19] Diffusion tensor (DT) tractography of the CST purely based on the supposed anatomic location, such as the presumed location of the PMA or in the cerebral peduncle, is not sufficient.[20] Both the location of the PMA and the CST, as well as the internal organization of the CST itself, have been shown to be variable in humans.[16,20,21] What is more important, the PMA and motor tracts may be displaced by a cerebral tumor and thus may not be present in the presumed location.[20,22] Therefore, anatomic landmarks may be insufficient to position the seed region of interest to visualize the CST and its most important subcomponents (ie, the hand and foot fibers). Besides that, edema and tumor infiltration can cause the diffusivity and anisotropy of the white matter tract to change,[23] compromising fiber tracking in these areas when one uses conventional parameter thresholds for termination of the tracking. The tracking of fibers in the vicinity of brain tumors, therefore, requires a custom-based approach, with more specific region-of-interest selection and optimization of parameter settings for DT tractography.

The aim of this feasibility study was to show that selecting

Received July 4, 2006; accepted after revision November 14.

From the Departments of Radiology (M.S., M.W.V., P.A.W., A.v.d.L.), Epidemiology and Biostatistics (M.W.V.), and Neurosurgery (A.J.P.E.V.), Erasmus MC, Rotterdam, the Netherlands; and ASL Europe (G.C.H.), GE Healthcare, Den Bosch, the Netherlands.

Both M.S. and M.W.V. contributed equally to this study.

Paper previously presented at: International Society for Magnetic Resonance in Medicine 14th Scientific Meeting, May 6–12, 2006; Seattle, Wash.

Please address correspondence to M.W. Vernooij, MD, Erasmus MC, Department of Radiology, PO Box 2040, 3000 CA Rotterdam; e-mail: m.vernooij@erasmusmc.nl

DOI 10.3174/ajnr.A0538

Table 1: Subject characteristics and fMRI tasks performed by each subject

Subject		Functional Neurologic Status		Type of Motor Task		
No./Sex/Age	Pathologic Diagnosis	Preoperative	Postoperative	Finger Tapping	Foot Tapping	Lip Pouting
1/F/27	N/A	N/A	N/A	L, R	L, R	Y
2/F/42	Anaplastic oligoastrocytoma	Severe left-sided hemiparesis	Unchanged	L, R		Y
3/M/56	High-grade oligodendroglioma	Minor left-sided hemiparesis	Unchanged	L, R	B	
4/F/55	Anaplastic oligoastrocytoma	No deficit	Minor left-sided hemiparesis	L, R		Y
5/F/48	WHO grade II astrocytoma	Minor paresis, left hand	Additional minor paresis, left leg	L, R	B	
6/F/31	Low-grade astrocytoma	No deficit	Subtle disturbances of fine motor skills, right hand	R		
7/M/44	Low-grade oligodendroglioma	No deficit	No deficit	L, R		
8/F/42	No certain pathologic diagnosis*	No deficit	No deficit	R	B	
9/F/35	Low-grade glioma	No deficit	Minor paresis, left hand	B	B	
10/M/59	Arteriovenous malformation	No deficit	No deficit	B		Y

Note:—F indicates female; M, male; N/A, not applicable (healthy volunteer); B, task performed on both sides simultaneously; R, task performed with right body side; L, task performed with left body side; Y, task performed; WHO, World Health Organization.
*Possibly resolving ischemic infarction.

fMRI activation areas as seed regions of interest for DT tractography yields useful preoperative information to evaluate the spatial relationship between the hand and foot fibers of the CST and the tumor borders.

Materials and Methods

Subjects

Ten subjects were included in this study. Table 1 presents the characteristics of the study subjects. To assess the feasibility of the study, we imaged 1 healthy volunteer. All other subjects ($n = 9$) were patients who required neurosurgery for an intracranial lesion. Eight patients were diagnosed with a primary intra-axial brain tumor, and 1 patient, with a symptomatic arteriovenous malformation. All patients were referred for preoperative assessment of the PMA and the CST. All brain lesions were located near the presumed location of the PMA and the CST. In all patients, neurosurgical excision of the intra-axial brain lesion was performed. Histopathologic examination confirmed the presence of a malignant tumor in 7 of the 8 patients with an expected malignancy. Clinical information on the patients' pre- and postoperative neurologic status was obtained from medical records and neurosurgical reports. The volunteer study received institutional review board approval, and written informed consent was obtained. Ethics committee approval was not required for the clinical work-up of the patients with tumor.

MR Imaging Data Acquisition

Imaging was performed on a 1.5T scanner (Signa CV/I; GE Healthcare, Milwaukee, Wis). An 8-channel head coil was used for reception of the signal intensity. For anatomic reference, a high-resolution T1-weighted 3D fast radio-frequency spoiled gradient-recalled acquisition in the steady state with an inversion-recovery prepulse sequence was used (TR/TE/TI, 9.9/2.0/400 ms; parallel imaging [ASSET] acceleration factor, 2; matrix, 320 × 224; FOV, 24 cm; section thickness, 1.6 mm; 86 contiguous sections). Acquisition time was 3:10 minutes. For functional imaging, a T2*-weighted gradient-echo echo-planar imaging (EPI) sequence was used (TR/TE, 3000/40 ms; matrix, 64 × 96; FOV, 24 cm; section thickness, 3.5 mm; 35 contiguous sections). Acquisition time was 5:15 minutes per functional run, including 5 dummy scans that were discarded from analysis. The DTI sequence was a single-shot diffusion-weighted spin-echo EPI sequence (TR/TE, 8000/68.7 ms; applying parallel imaging [array special sensitivity encoding technique] with acceleration factor 2; matrix, 96 × 64; FOV, 21 cm; section thickness, 3.5 mm; 38 contiguous sections). Maximum b value was 1000 s/mm^2 in 25 noncollinear directions. Acquisition time was 3:44 minutes.

fMRI Stimulation Paradigm

The stimulation paradigm consisted of a blocked design of finger tapping, foot tapping, or lip pouting versus rest (30 seconds per block; 10 blocks per scanning session). Finger tapping was performed either with the right or the left hand separately or with both hands simultaneously and consisted of self-paced consecutive opposition of the thumb to each of the other fingers of the hand. Foot tapping was always performed with both feet simultaneously and consisted of self-paced dorsal and plantar flexion of the feet. The lip motor task consisted of self-paced repetitive lip pouting. Subjects were instructed to perform each of the tasks consciously and to limit head motion. During the rest condition, the subject was instructed to stop performing the task and to relax. Instructions "start" and "rest" were presented auditorily at the start of the active and rest conditions, respectively.

Table 1 gives an overview of the fMRI tasks performed by each subject. The choice of motor tasks to be performed by the subject was based on the location of the tumor and its presumed proximity to the PMA. Irrespective of tumor location, a finger-tapping task with real-time analysis is routinely performed at the start of each fMRI examination in our department, to enable assessment of possible limitations of the fMRI examination (eg, due to medication, poor comprehension/cooperation, and so forth). Each subject performed a minimum of 1 and a maximum of 5 tasks.

fMRI and DTI Data Processing and Analysis

Data processing and analysis of fMRI data were performed off-line. Statistical analysis of the fMRI data was performed by using Statistical Parametric Mapping, Version 2 (SPM2; Wellcome Department, University College, London, UK). The T2*-weighted functional images were realigned to correct for the subject's motion during data acquisition.[24]

Functional and anatomic images were then coregistered with the DTI images. Functional data were smoothed with a 3D Gaussian filter of 6 × 6 × 6 mm^3 full width at half maximum; no normalization was performed. Individual statistical parametric maps were calculated by using the general linear model by modeling the "active" and "rest" conditions as a boxcar function convolved with the hemodynamic

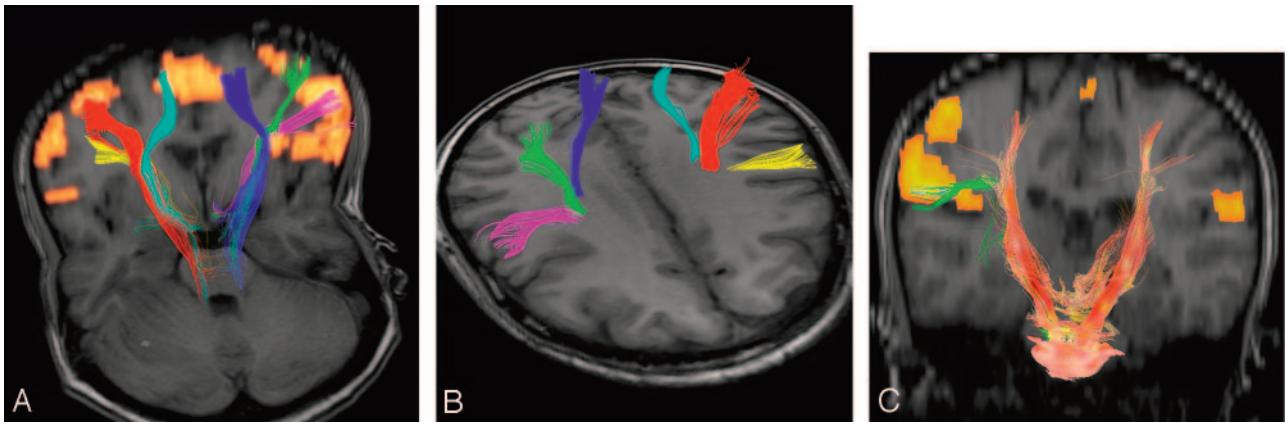

Fig 1. Orthogonal axial/coronal (*A*) and axial (*B*) projection of T1-weighted MR images with fiber tracts depicted in color in the healthy volunteer (violet and yellow, lip fibers; green and red, hand fibers; pale blue and dark blue, foot fibers) The hand and foot fibers of the corticospinal and the lip fibers of the corticobulbar tract can be clearly distinguished and visualized (*A* and *B*). The different fMRI activation areas used to choose the seed regions of interest are shown in color (*A*). The course of the fibers through the corona radiata follows the known somatotopic distribution (*B*). *C*, The results are shown from conventional DT tractography (in orange) as well as from fMRI-based fiber tracking with region-of-interest placement in the PMA of the lip of the right hemisphere (in green), projected on a coronal T1-weighted image of the healthy volunteer. fMRI activation (shown in yellow-orange) is visible in the PMA of the lip and supplementary motor area in both images. Clearly, the lip fibers are only visualized by using the fMRI-based fiber tracking approach and not with the conventional fiber tracking approach.

response function. A t-contrast was then calculated for the "active" minus the "rest" condition.

DTI data were processed and analyzed off-line. DT tractography was performed with the freely available software dTV for MR-DTI analysis (University of Tokyo Hospital, Tokyo, Japan) by using the fiber assignment by continuous tracking (FACT) method.[14,25] Both the DTI and the fMRI data were loaded into the software package, which enabled us to perform seed region-of-interest selection driven by the locations of the coregistered fMRI activations.

To compare fiber tracking by means of this fMRI-based seed region-of-interest placement with the more conventional fiber tracking approach by using region-of-interest placement based on anatomic landmarks only, we performed DT tractography with these 2 approaches in all subjects.

For the fMRI-based approach, fiber tracking was initiated in both retrograde and antegrade directions from a manually selected freeform seed region of interest that was chosen in the white matter area immediately subjacent to the maximal fMRI activity in the precentral cortical gray matter. The entire cerebral peduncle was chosen as a target region of interest. For the conventional fiber tracking approach, a freeform seed region of interest was manually placed in the entire cerebral peduncle, from which fiber tracking was initiated in both retrograde and antegrade directions. The cerebral peduncle is an anatomically well-known and reliable location of the CST that was least likely to be influenced by potential mass effect of intra-axial lesions. For the conventional fiber-tracking approach, we chose not to use a target region of interest, placed, for example, in the internal capsule or PMA, because these areas were often displaced by the mass effect of the lesion, which would render region-of-interest placement unreliable. For both approaches, diffusion tensors, eigenvalues, and eigenvectors were computed from linearly interpolated diffusion tensor images at each iteration, and tracking was terminated when it reached given threshold values of fractional anisotropy (FA) and angle (60°) between consecutive vector lines. The FA threshold was by default 0.20, but it was lowered in cases in which no tract was visualized by using the default settings, because the FA values in the tract could be decreased by the edema and/or tumor infiltration. The tracked fibers were assessed in 3D by using multiple orthogonal projections overlaid on the high-resolution T1-weighted images, to determine their actual and apparent relationships to the brain tumor.

Results

Volunteer

In the healthy volunteer (subject 1), the PMA of the hand, foot, and lip on both sides was successfully established by fMRI. By using fMRI-driven seed regions of interest, we could clearly visualize and distinguish fiber tracts of the hand, foot, and lip on both sides (Fig 1*A*, -*B*). Each tract followed a distinct course through the corona radiata and internal capsule with hand fibers coursing anterior and lateral to foot fibers and lip fibers showing the most anterolateral trajectory (Fig 1*B*).

In contrast, when the conventional fiber tracking approach was used, the lip fibers were not visualized (Fig 1*C*). Also, the CST fibers were not visualized as far along their course toward the PMA as they were with the fMRI-based fiber tracking approach.

Patients

The PMA could be established with fMRI for all motor tasks of interest in all patients. Table 1 shows that all patients performed finger tapping on at least 1 side; additionally, 4 patients performed foot tapping and 3 patients performed lip pouting.

fMRI-Based DT Tractography Versus Conventional DT Tractography

In all 9 patients, we were able to track the hand fibers of the CST from all PMAs by using the fMRI-based seed region-of-interest approach. In the 4 patients who also performed foot tapping, we could make a clear distinction between the hand and foot fibers. Of the 3 patients who performed lip pouting, the corticobulbar fibers of the lip could be tracked by using fMRI-based seed regions of interest on both sides in 1 patient (subject 10) and on the nontumor side in the other 2 patients (subjects 2 and 4, images not shown).

With the conventional fiber tracking approach, lip fibers

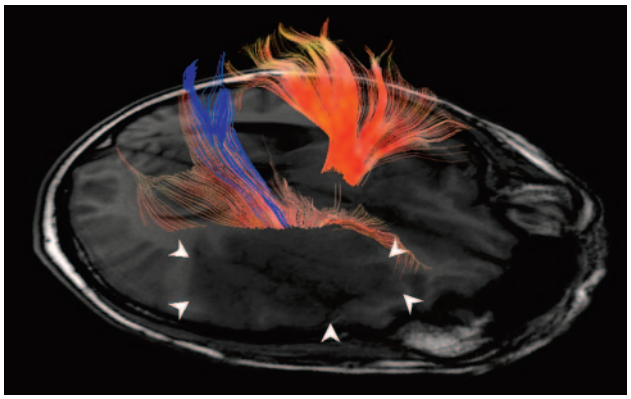

Fig 2. Axial T1-weighted MR image of a patient with a brain tumor with fibers of the corticospinal tract projected in color. Results from conventional fiber tracking based on anatomic landmarks (in orange) show dispersion and diminished visualization of the CST fibers in the hemisphere affected by the lesion (*arrowheads*), compared with the unaffected hemisphere. DT tractography based on seed region-of-interest selection in the PMA of the hand as established with fMRI shows, in blue, the CST fibers of the hand in the affected hemisphere, allowing a clear demarcation of the fibers of interest within the CST.

were not visualized in any of the patients. The hand and foot fibers could not be distinguished within the internal capsule or corona radiata, nor could the CST fibers be visualized as far along their course toward the PMA as with the fMRI-based fiber-tracking approach. Furthermore, in 3 patients (subjects 2, 3, and 4), the CST fibers were markedly dispersed, scarce, and prematurely terminated in the hemisphere with the lesion, compared with the nonaffected hemisphere (Fig 2).

fMRI-Based DT Tractography and Clinical Correlates

In 3 patients (subjects 2, 3, and 6), the PMA of the hand and/or foot as shown on fMRI was displaced by the tumor (Table 2). The tracked CST in these patients was also displaced compared with the other side (Fig 3). In 2 of these patients (subjects 2 and 3), functional neurologic deficit was present preoperatively (Table 1). All 3 patients underwent awake neurosurgical resection of the lesion, during which electrocortical mapping was performed, confirming the proximity of the lesion to the PMA in each case. Postoperatively, the functional neurologic status had remained unchanged in both patients with a pre-existing deficit. In 1 patient (subject 6), subtle disturbances of the fine motor skills of the right hand had developed after resection of the tumor that was located in close proximity to the PMA of the right hand.

In 2 patients (subjects 3 and 5), both the PMA and the CST were located in areas of decreased signal intensity on the T1-weighted images (due to perifocal edema or tumor infiltration, Fig 4). At conventional fiber tracking FA thresholds (0.20), these fiber tracts were not visible. Only by using a lower FA threshold could these tracts be visualized (Fig 5*A–C*). Both patients had preoperative neurologic deficits (Table 1), and in both patients, neurosurgical resection of the lesion aided by electrocortical stimulation was performed. The functional neurologic status had remained unchanged in 1 patient (subject 3). In the other patient (subject 5), a minor paresis of the left leg had developed postoperatively in addition to pre-existing minor paresis of the left hand. As shown by DT tractography, the CST fibers of this patient's left leg ran through an area of perifocal edema or tumor infiltration (Fig 5).

In 1 patient (subject 4), the PMA of the hand was at a considerable distance from the tumor. fMRI-based DT tractography in this patient, however, showed that the hand fibers ran adjacent to the tumor border. This patient, with no preexisting neurologic deficit, developed an ischemic stroke due to increased intracranial pressure postoperatively and was eventually left with a minor left-sided hemiparesis (Table 1). Intraoperative electric mapping had not indicated proximity of the tumor to eloquent brain regions.

In 4 patients (subjects 7–10), both the PMA and the tracked fibers showed no relation to the tumor border, though in 3 of these patients (subjects 7, 8, and 9), the lesion was in close proximity to the supplementary motor area. In these 3 patients, electrocortical mapping was performed intraoperatively, whereas in the remaining patient (subject 10), the lesion was neurosurgically resected with the patient under general anesthesia (ie, without electrocortical mapping). All of these patients were neurologically intact preoperatively. In 1 patient (subject 9), minor paresis of the left hand had developed postoperatively (Table 1).

Discussion

We showed that incorporating the fMRI-assessed information on cortical activation areas into DT tractography for fiber tracking of the motor tracts is feasible not only in the healthy brain but also when intra-axial lesions are present. In the preoperative assessment of patients with brain tumors, this can provide essential information not only on the location of eloquent cortical areas but also on the course of important subcortical white matter tracts. This information cannot be obtained from conventional anatomic MR imaging or from conventional DT tractography based on anatomic landmarks.

The integration of both high-resolution anatomic (T1-weighted) data with fMRI data in the fiber-tracking procedure makes an evaluation of the spatial relationship between tracked fibers and tumor borders possible. Also, this coregistration of anatomic, functional, and DTI data facilitates the potential intraoperative use of the data, for example in devices for stereotactic surgical navigation.

In contrast to intraoperative cortical mapping, the electric stimulation of the subcortical white matter during surgery is not very successful for reliably identifying functional white matter tracts.[26,27] Also, in deep subcortical tumors, the normal position of the PMA may be preserved, whereas only the CST or a few fiber bundles of the CST may be displaced.[28] In such cases, the PMA cannot be used as a landmark for the CST. Therefore, a method to noninvasively visualize the important fiber tracts and their subcomponents would be of great benefit for presurgical planning and guiding the operative procedure. We showed that tracking of the CST directly from the fMRI activation area can be used to visualize and distinguish the different components of the CST, especially the hand and foot fibers. In a healthy volunteer, the presented method showed that the tracked hand, foot, and lip fibers follow a distinct course, the foot fibers coursing posteromedially to the hand fibers within the posterior limb of the internal capsule (PLIC).[16,28,29] This distribution within the corticospinal tract confirmed previous findings by Holodny et al,[16] who also studied the CST by using DT tractography and found the same location and internal organization of the separate CST components within the PLIC. Both our study and that of Holodny

Table 2: Overview of the most important findings by fMRI and DT tractography in each subject

No.	PMA on fMRI	Fiber Tracts on fMRI-Driven DT Tractography
1	Healthy volunteer: PMAs of hand, foot, and lip on both sides at known anatomic position	Hand, foot, and lip fibers on both sides at known anatomic position
2	PMA of hand displaced laterally and caudally by tumor	Hand fibers on tumor side displaced compared with healthy side, visualization of lip fibers only on healthy side
3	PMA of hand and foot displaced by tumor and in area of decreased signal intensity on T1WI	Hand and foot fibers displaced on tumor side, run through area of altered signal intensity on T1WI
4	PMA at distance from lesion	Hand fibers run very close to tumor border, lip fibers visualized only on healthy side
5	PMA of hand and foot in area of altered signal intensity on T1WI, near tumors	Hand fibers normal course, foot fibers run through area of altered signal intensity on T1WI, close to tumor
6	PMA of hand displaced cranially and dorsally	Hand fibers displaced by tumor
7	PMA not displaced and not related to tumor border	Hand fibers not displaced
8	PMA not displaced and not related to tumor border	Hand and foot fibers not displaced
9	PMA not displaced and not related to tumor border	Hand and foot fibers not displaced
10	PMA not displaced and not related to AVM border	Hand fibers not displaced, visualization of lip fibers on both sides

Note:—T1WI indicates T1-weighted images; AVM, arteriovenous malformation.

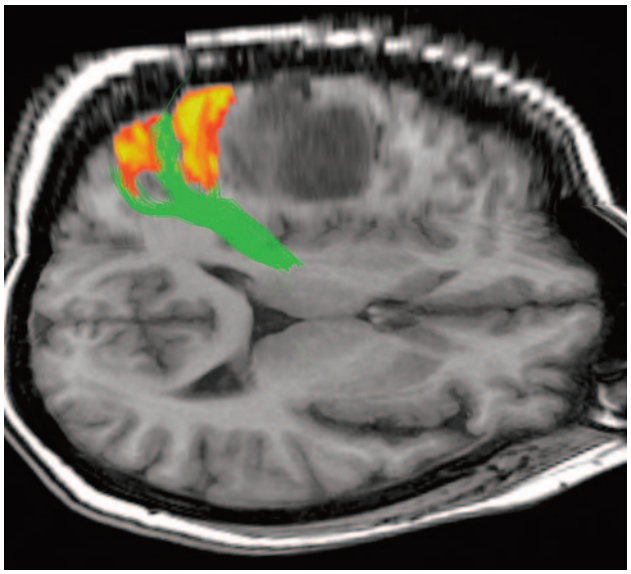

Fig 3. Orthogonal axial/sagittal projection of a T1-weighted MR image with overprojection of the hand PMA and the hand fibers of the CST. In this patient, the left PMA, as shown by fMRI (in orange-yellow), was displaced by tumor, as was the tracked CST (in green).

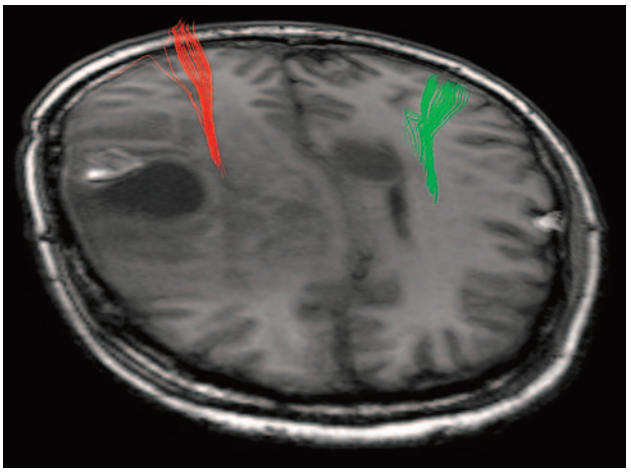

Fig 4. Axial T1-weighted MR image with fiber tracts projected in color (red and green for the right and left hemispheres, respectively). In this patient, hand fibers ran through an area of altered signal intensity, due to edema or tumor infiltration.

et al indicate that the hand and foot fibers are organized along the short (left-right) axis of the PLIC, rather than along the long (anteroposterior) axis of the PLIC, as has been previously assumed.[30]

In patients with a brain tumor, the (deviated) course of the white matter tract and its relationship to the tumor may be depicted by our integrated fMRI–DT tractography method. This is extremely useful in cases in which the PMA is located away from the tumor, but the CST runs closely by the tumor area. We showed that tracking the CST based only on anatomic landmarks may not be sufficient to visualize reliably the CST and that fMRI-based seed region-of-interest placement may be necessary to visualize the CST in its entirety. With fMRI-based DT tractography, the CST fibers could be followed farther along their course toward the PMA than when DT tractography was performed on the basis of anatomic landmarks only. Furthermore, DT tractography of the CST was seen to be hampered in cases of anatomic distortion due to a mass effect of the lesion or in cases of altered diffusivity due to tumor infiltration or perifocal edema in the region of the CST. Tracking improved when the fMRI-based seed region-of-interest approach was used, thus providing more reliable preoperative information.

Recently, other authors have described methods to combine the information on functional cortical areas assessed by fMRI with information on the course of the CST as visualized by DT tractography.[20,22,31-33] However, to our knowledge, only 2 studies used a real fMRI-based seed region-of-interest selection procedure for fiber tracking, and these were limited only to identifying the hand fibers within the CST.[20,31] Not only have we identified the hand fibers but our method was also successful in distinguishing other fibers both in a healthy volunteer and in patients with tumor, by using fMRI-based region-of-interest selection. This distinction may provide additional presurgical information, in particular allowing a more specific risk estimate before neurosurgical resection of a lesion as well as guiding electric stimulation of the subcortical white matter intraoperatively. Within the CST, the hand and foot fibers run together, such that they are indistinguishable with DT tractography without the placement of a region of interest in a location specific to each of these fibers.[16] Although the known somatotopic distribution within the precentral gyrus may allow specific region-of-interest placement in the PMAs

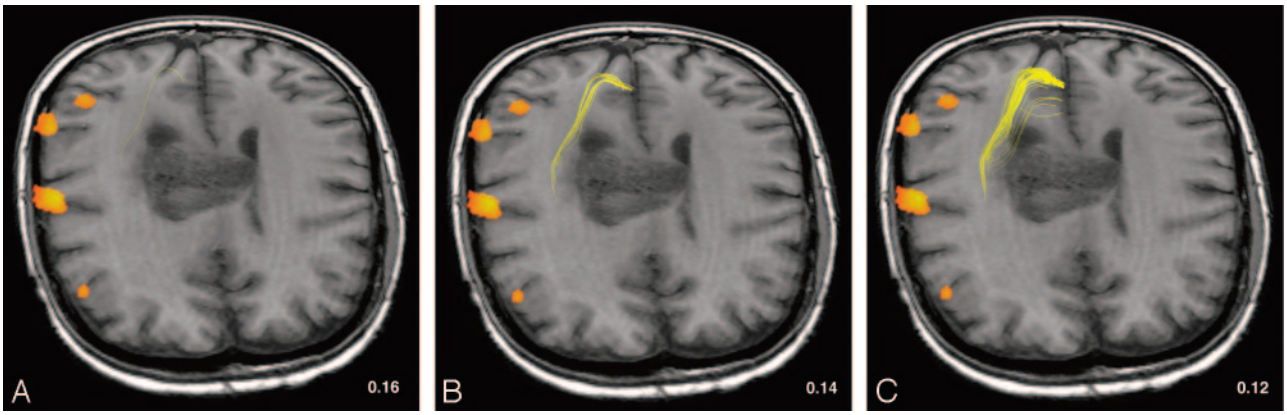

Fig 5. Axial T1-weighted MR images with foot fibers projected in color. Fibers pass through an area of altered signal intensity on T1-weighted images. Varying the FA thresholds for fiber tracking in this patient had a considerable influence on the fibers depicted (*A–C*, FA thresholds used are shown in each image).

of the hand or the foot in healthy volunteers based on structural anatomic images only, distortion by a mass effect of the lesion renders this approach unreliable in patients with brain tumor.[20,22] With fMRI, the PMAs are accurately identified,[3-5] and this information allows reliable region-of-interest placement in the hand and foot PMAs within the precentral gyrus. The possibility of distinguishing the hand and foot fibers within the CST is not only relevant in the preoperative assessment of patients with brain tumors but could also be extended to other clinical situations, for example, for planning functional neurosurgery in patients with Parkinson disease and related disorders.

A further strength of our study lies in the clinical applicability of our protocol. The DTI sequence that we used is clinically feasible, with an acquisition time of only 3:44 minutes. Standard presurgical clinical fMRI examinations in patients with brain tumors usually take approximately 20–30 minutes for a protocol consisting of 3–4 motor tasks, including an anatomic T1-weighted scan. The addition of a short DTI sequence takes relatively little time, does not require active patient participation, and may yield important additional information.

Several limitations, however, need to be considered. First, we performed the fMRI and DT tractography combined method in only 1 healthy volunteer and 9 patients. Although this is a limited number of subjects, the fact that the method was successful in distinguishing hand and foot fibers in all cases attests to its robustness and demonstrates its validity for subjects with variable tumor size and location.

Second, we could not identify all lip fibers on the tumor side in the subjects who performed lip pouting. Previous studies suggest that fiber tracking of the motor tracts is inadequate in the lateral portions of the corticobulbar/spinal tract,[34,35] such as the mouth and tongue fiber tracts, and that these tracts can, therefore, not be successfully mapped by DT tractography. Holodny et al[36] reported that the corticobulbar tract (CBT) is probably too small to trace because when fibers cross, the fiber tracking algorithm will preferentially track the larger tract (ie, the CST or the longitudinal fasciculus). However, Thomas et al[37] successfully tracked the CBT in 5 patients with hemiparetic cerebral palsy in both hemispheres, by placing regions of interest in the internal capsule and in the cerebral peduncle and pons and by optimizing the angular deflection threshold.

Although not successful in all patients on the tumor side, our results in a healthy volunteer and 3 patients also demonstrate that tracking of lip fibers is feasible. One possible explanation for the fact that we succeeded in tracking the CBT in our subjects is that we chose a specific region of interest on the basis of the fMRI activation in the cortex and did not track from a region of interest placed in the cerebral peduncle.

As mentioned previously, the single tensor-fitting algorithm often fails at major fiber crossings due to intravoxel averaging of tensor direction.[14,38,39] fMRI-based seed region-of-interest placement in itself does not eliminate this problem. However, the main problem with tracking the CBT lies in the fact that it runs together with the CST until it takes a relatively sharp turn at the level just dorsal to the internal capsule. Not only will FA values be reduced at the point where the 2 tracts branch (due to intravoxel tensor direction averaging) but also has the CBT branch a sharply deflecting course. Both of these issues may cause the single tensor-fitting algorithm to fail when one attempts to track the CBT from a seed region of interest placed in the cerebral peduncle, for instance, because intravoxel tensor-direction averaging will favor the course of the larger CST and angle deflection is restricted within, for example, the FACT algorithm. The branching problem is much more easily handled by merging 2 lines instead of splitting a line into 2.[14] In the case of tracking the CBT, merging 2 lines is achieved by initiating fiber tracking of the CBT from a seed region of interest in the primary motor area of the lip, while further constraining its course by a target region of interest in the cerebral peduncle. Our findings demonstrate that the visualization of motor tract components other than hand and foot fibers is possible when basing it on fMRI activation areas.

The inability of the tracking algorithm to detect lip fibers in the tumor hemisphere of 2 patients may reflect the interaction of at least 2 complications. First, fiber tracking is dependent on the diffusion characteristics of the white matter tracts, which will inevitably change during lesion formation (see next paragraph), either due to underlying physiologic change or separation of fiber bundles resulting in enhanced partial volume effects. Second, it is possible that the lip fibers were deviated by

the tumor in such a way that they ran at too sharp an angle to be tracked by the algorithm used here.

Tracking results were found to vary according to the FA threshold. Edema and tumor infiltration typically cause reduction of the FA measured in these voxels.[23,34] This can cause significant problems in fiber tracking, with fibers terminating prematurely due to crossing the chosen minimal FA threshold.[20] The optimal tractability threshold of FA for DT tractography of the CST is commonly considered to be around 0.20.[40] However, this number was derived from patients with stroke and motor deficits, who only showed minor decrease in FA in the affected CST. Lowering the FA threshold for fiber tracking, on the other hand, is expected to introduce erroneous false-positive fiber tracts, in particular when only 1 seed region of interest is used.[14,40] With multiple regions of interest such as we used, the amount of false-positive fiber tracts is reduced by constraining the tract reconstruction,[14] which makes lowering of FA thresholds, in cases of changed diffusivity due to perifocal edema or tumor infiltration, possible without introducing many erroneous tracts. We show that DT tractography in patients with tumor in a clinical setting needs to be customized because the area of the CST may be edematous or infiltrated by tumor; thus, an FA termination threshold that is set too high may lead to failure of fiber tracking (Fig 4). Specific fMRI-based region-of-interest placement, such as we propose, provides additional a priori information for the tracking and subsequent visualization of the course of the tract and, therefore, facilitates decreasing the FA threshold when required.

The impact of using the proposed integration of fMRI and DT tractography on clinical practice was not formally assessed. Studies formally assessing the impact of implementation of fMRI alone in clinical practice are still scarce,[41,42] and as far as we are aware, none discuss the integration of fMRI and DT tractography in the preoperative assessment of patients with brain tumors. In fact, the combined use of fMRI and DTI is far from being implemented in routine clinical practice as yet, and even though very promising for clinical practice,[13] its feasibility still needs to be further assessed. Once feasibility of functional imaging by using the combination of fMRI and DTI has been shown, such as in ours and in previous studies,[43] future studies formally evaluating the impact of the combined use of fMRI and DTI on clinical practice, in terms of therapeutic and clinical decision-making, neurosurgical procedures, and patient outcomes will be needed. This will be greatly facilitated when full integration of functional imaging data with surgical neuronavigation systems is established.

One could argue that fiber tracking, as described in our study, is time-intensive and operator-dependent. However, DT tractography postprocessing time can be decreased by a more standardized choice of the (seed) region of interest and increasing experience with the technique. The choice of the region of interest we propose is less operator-dependent than that in other studies because the region of interest to be chosen does not require a good knowledge of the anatomic location of various white matter tracts because in our study, it is based on the fMRI activation area. Additional postprocessing time is not prohibitive if one considers the clinical implications described previously. The fMRI postprocessing for a preoperative assessment of the PMA alone generally takes approximately 1 hour. This includes the time required for coregistration of the functional and anatomic images to the DTI data, which is not different from conventional fMRI postprocessing when, instead of being coregistered to the DTI data, the functional images are coregistered to the anatomic data. The additional postprocessing time for DTI data needed in our study was approximately 20 minutes. Future incorporation of the visualized fiber tracts in neuronavigation equipment may further enhance the clinical usefulness.

Conclusion

We propose a clinically feasible protocol of integrating fMRI and DT tractography to optimize the presurgical assessment of the cortical motor areas and subcortical white matter tracts in patients with brain tumors. fMRI-based DT tractography is superior to DT tractography on the basis of anatomic landmarks alone, because only with fMRI-based DT tractography is a distinction between the several components of the CST possible. Furthermore, it allows decreasing the FA threshold if necessary and provides an improved visualization of the CST, in particular when fiber tracking is hampered by the presence of tumor or perifocal edema.

References

1. Sunaert S, Yousry TA. **Clinical applications of functional magnetic resonance imaging.** *Neuroimaging Clin N Am* 2001;11:221–36, viii
2. Haughton VM, Turski PA, Meyerand B, et al. **The clinical applications of functional MR imaging.** *Neuroimaging Clin N Am* 1999;9:285–93
3. Yousry TA, Schmid UD, Jassoy AG, et al. **Topography of the cortical motor hand area: prospective study with functional MR imaging and direct motor mapping at surgery.** *Radiology* 1995;195:23–29
4. Yetkin FZ, Mueller WM, Morris GL, et al. **Functional MR activation correlated with intraoperative cortical mapping.** *AJNR Am J Neuroradiol* 1997;18:1311–15
5. Pujol J, Conesa G, Deus J, et al. **Presurgical identification of the primary sensorimotor cortex by functional magnetic resonance imaging.** *J Neurosurg* 1996;84:7–13
6. Schulder M, Maldjian JA, Liu WC, et al. **Functional image-guided surgery of intracranial tumors located in or near the sensorimotor cortex.** *J Neurosurg* 1998;89:412–18
7. Mueller WM, Yetkin FZ, Hammeke TA, et al. **Functional magnetic resonance imaging mapping of the motor cortex in patients with cerebral tumors**. *Neurosurgery* 1996;39:515–20
8. Laundre BJ, Jellison BJ, Badie B, et al. **Diffusion tensor imaging of the corticospinal tract before and after mass resection as correlated with clinical motor findings: preliminary data.** *AJNR Am J Neuroradiol* 2005;26:791–96
9. Basser PJ, Jones DK. **Diffusion-tensor MRI: theory, experimental design and data analysis: a technical review.** *NMR Biomed* 2002;15:456–67
10. Pierpaoli C, Jezzard P, Basser PJ, et al. **Diffusion tensor MR imaging of the human brain.** *Radiology* 1996;201:637–48
11. Nimsky C, Ganslandt O, Hastreiter P, et al. **Preoperative and intraoperative diffusion tensor imaging-based fiber tracking in glioma surgery.** *Neurosurgery* 2005;56:130–38
12. Nimsky C, Ganslandt O, Merhof D, et al. **Intraoperative visualization of the pyramidal tract by diffusion-tensor-imaging-based fiber tracking.** *Neuroimage* 2006;30:1219–29
13. Ulmer JL, Salvan CV, Mueller WM, et al. **The role of diffusion tensor imaging in establishing the proximity of tumor borders to functional brain systems: implications for preoperative risk assessments and postoperative outcomes.** *Technol Cancer Res Treat* 2004;3:567–76
14. Mori S, van Zijl PC. **Fiber tracking: principles and strategies—a technical review.** *NMR Biomed* 2002;15:468–80
15. Jones DK, Simmons A, Williams SC, et al. **Non-invasive assessment of axonal fiber connectivity in the human brain via diffusion tensor MRI.** *Magn Reson Med* 1999;42:37–41
16. Holodny AI, Gor DM, Watts R, et al. **Diffusion-tensor MR tractography of somatotopic organization of corticospinal tracts in the internal capsule: initial anatomic results in contradistinction to prior reports.** *Radiology* 2005;234:649–53
17. Catani M, Howard RJ, Pajevic S, et al. **Virtual in vivo interactive dissection of white matter fasciculi in the human brain.** *Neuroimage* 2002;17:77–94
18. Akai H, Mori H, Aoki S, et al. **Diffusion tensor tractography of gliomatosis**

cerebri: fiber tracking through the tumor. *J Comput Assist Tomogr* 2005;29:127–29
19. Stieltjes B, Kaufmann WE, van Zijl PC, et al. **Diffusion tensor imaging and axonal tracking in the human brainstem.** *Neuroimage* 2001;14:723–35
20. Schonberg T, Pianka P, Hendler T, et al. **Characterization of displaced white matter by brain tumors using combined DTI and fMRI.** *Neuroimage* 2006;30: 1100–11. Epub 2006 Jan 19
21. Burgel U, Amunts K, Hoemke L, et al. **White matter fiber tracts of the human brain: three-dimensional mapping at microscopic resolution, topography and intersubject variability.** *Neuroimage* 2006;29:1092–105
22. Parmar H, Sitoh YY, Yeo TT. **Combined magnetic resonance tractography and functional magnetic resonance imaging in evaluation of brain tumors involving the motor system.** *J Comput Assist Tomogr* 2004;28:551–56
23. Field AS, Alexander AL, Wu YC, et al. **Diffusion tensor eigenvector directional color imaging patterns in the evaluation of cerebral white matter tracts altered by tumor.** *J Magn Reson Imaging* 2004;20:555–62
24. Friston KJ, Williams S, Howard R, et al. **Movement-related effects in fMRI time-series.** *Magn Reson Med* 1996;35:346–55
25. Mori S, Crain BJ, Chacko VP, et al. **Three-dimensional tracking of axonal projections in the brain by magnetic resonance imaging.** *Ann Neurol* 1999;45:265–69
26. Lang FF, Olansen NE, DeMonte F, et al. **Surgical resection of intrinsic insular tumors: complication avoidance.** *J Neurosurg* 2001;95:638–50
27. Holodny AI, Schwartz TH, Ollenschleger M, et al. **Tumor involvement of the corticospinal tract: diffusion magnetic resonance tractography with intraoperative correlation.** *J Neurosurg* 2001;95:1082
28. Ebeling U, Reulen HJ. **Subcortical topography and proportions of the pyramidal tract.** *Acta Neurochir (Wien)* 1992;118:164–71
29. Bertrand G, Blundell J, Musella R. **Electrical exploration of the internal capsule and neighbouring structures during stereotaxic procedures.** *J Neurosurg* 1965;22:333–43
30. Gray H. **Neurology.** In: Williams P, Warwick R, Dyson M, et al., eds. *Gray's Anatomy.* Edinburgh, UK: Livingstone; 1989:1073
31. Holodny AI, Ollenschleger MD, Liu WC, et al. **Identification of the corticospinal tracts achieved using blood-oxygen-level-dependent and diffusion functional MR imaging in patients with brain tumors.** *AJNR Am J Neuroradiol* 2001;22:83–88
32. Guye M, Parker GJ, Symms M, et al. **Combined functional MRI and tractography to demonstrate the connectivity of the human primary motor cortex in vivo.** *Neuroimage* 2003;19:1349–60
33. Kamada K, Sawamura Y, Takeuchi F, et al. **Functional identification of the primary motor area by corticospinal tractography.** *Neurosurgery* 2005;56:98–109
34. Clark CA, Barrick TR, Murphy MM, et al. **White matter fiber tracking in patients with space-occupying lesions of the brain: a new technique for neurosurgical planning?** *Neuroimage* 2003;20:1601–08
35. Hagmann P, Thiran JP, Jonasson L, et al. **DTI mapping of human brain connectivity: statistical fibre tracking and virtual dissection**. *Neuroimage* 2003;19:545–54
36. Holodny AI, Watts R, Korneinko VN, et al. **Diffusion tensor tractography of the motor white matter tracts in man: current controversies and future directions.** *Ann N Y Acad Sci* 2005;1064:88–97
37. Thomas B, Eyssen M, Peeters R, et al. **Quantitative diffusion tensor imaging in cerebral palsy due to periventricular white matter injury.** *Brain* 2005;128:2562–77
38. Jones DK, Pierpaoli C. **Confidence mapping in diffusion tensor magnetic resonance imaging tractography using a bootstrap approach.** *Magn Reson Med* 2005;3:1143–49
39. Parker GJ, Alexander DC. **Probabilistic anatomical connectivity derived from the microscopic persistent angular structure of cerebral tissue.** *Philos Trans R Soc Lond B Biol Sci* 2005;360:893–902
40. Kunimatsu A, Aoki S, Masutani Y, et al. **The optimal trackability threshold of fractional anisotropy for diffusion tensor tractography of the corticospinal tract.** *Magn Reson Med Sci* 2004;3:11–17
41. Petrella JR, Shah LM, Harris KM, et al. **Preoperative functional MR imaging localization of language and motor areas: effect on therapeutic decision making in patients with potentially resectable brain tumors.** *Radiology* 2006;240:793–802
42. Medina LS, Bernal B, Dunoyer C, et al. **Seizure disorders: functional MR imaging for diagnostic evaluation and surgical treatment—prospective study.** *Radiology* 2005;236:247–53
43. Nimsky C, Grummich P, Sorensen AG, et al. **Visualization of the pyramidal tract in glioma surgery by integrating diffusion tensor imaging in functional neuronavigation.** *Zentralbl Neurochir* 2005;66:133–41